Negron et al.,: supplementary information

SI.1 Calibration of the bioaerosol sampler flow rate

The flow rate of air sampled by the SpinCon II was calibrated with a VT100 Hotwire Thermo-anemometer (Cole Palmer Inc.), attached to a tube temporarily mounted on the sampler inlet while the instrument was in operation. Several measurements of flow velocity were taken from 3 ports (Figure S1, Holes 1-3) so that the anemometer tip was located at the center of the tube (green dot in Figure S1). The high flow rate ensures that highly turbulent conditions exist in the tube, so that the axial velocity, U, varies little in the radial direction. The volumetric flow rate, Q, is then obtained from U as:

$$Q = (\frac{\pi}{4})(ID)^2 U \quad [S1]$$

where ID is the inner diameter of the tube. The average volumetric flow rate was 478 ± 6 L min^{-1}, which represents a 6% difference to the 450 L min^{-1} flow rate reported by InnovaPrep Inc.

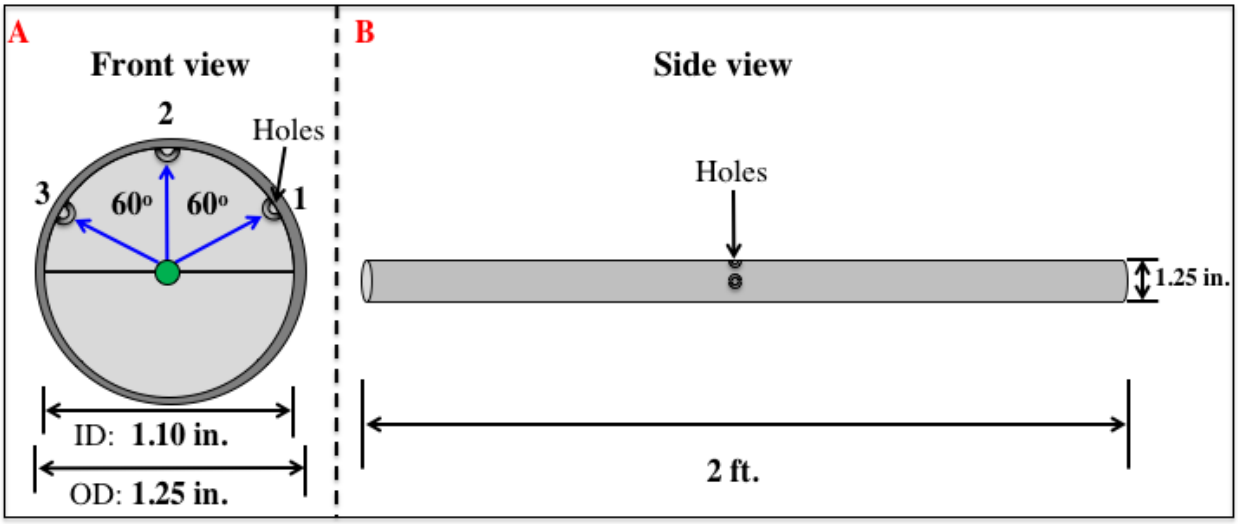

Figure S1: Tube design used to perform volumetric flow rate measurements of the SpinCon II; a) shows the front view of the tube with the description of the holes where measurements were taken with the hotwire anemometer, and b) shows the side view of the tube.

SI.2 Setting FL1- A threshold determination procedure

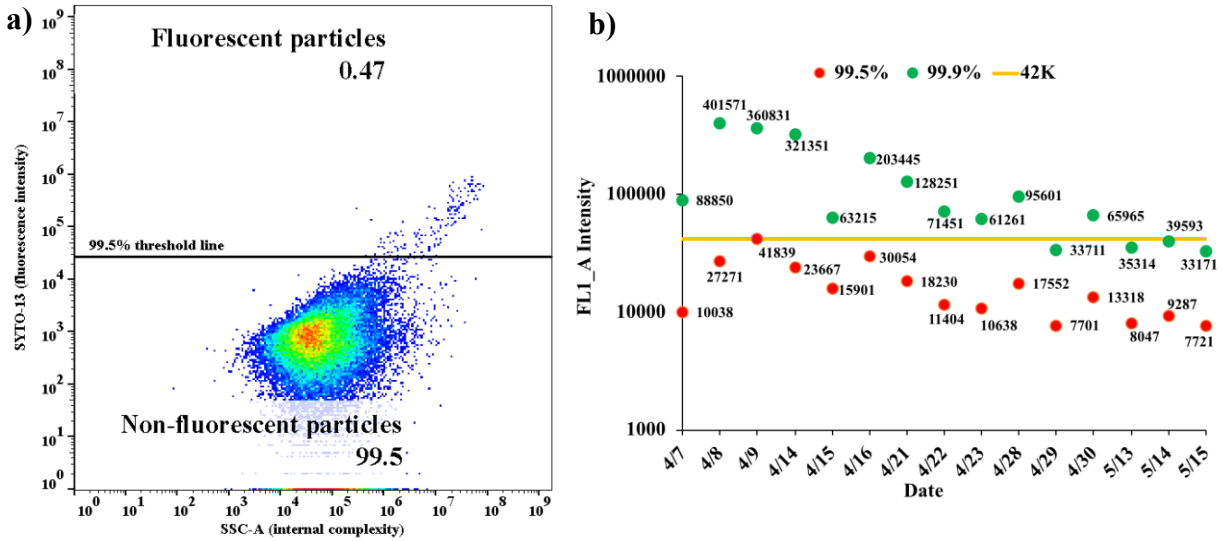

Figure S2: Threshold approach applied to atmospheric samples: (a) April 14, 2015 atmospheric sample blank (no SYTO-13) FL1-A vs. SSC-A plot showing the threshold value (line) to constrain 99.5% of autofluorescent particles (line, FL1_A value: 24k), and (b) summarize the 99.5% and 99.9% calculated values(Y-axis: FL1_A intensity) for each sampling event (x-axis: sampling day in month/day format), and the 42k (41839 units) threshold chosen (yellow line).

SI.3 FCM contour plots and gating

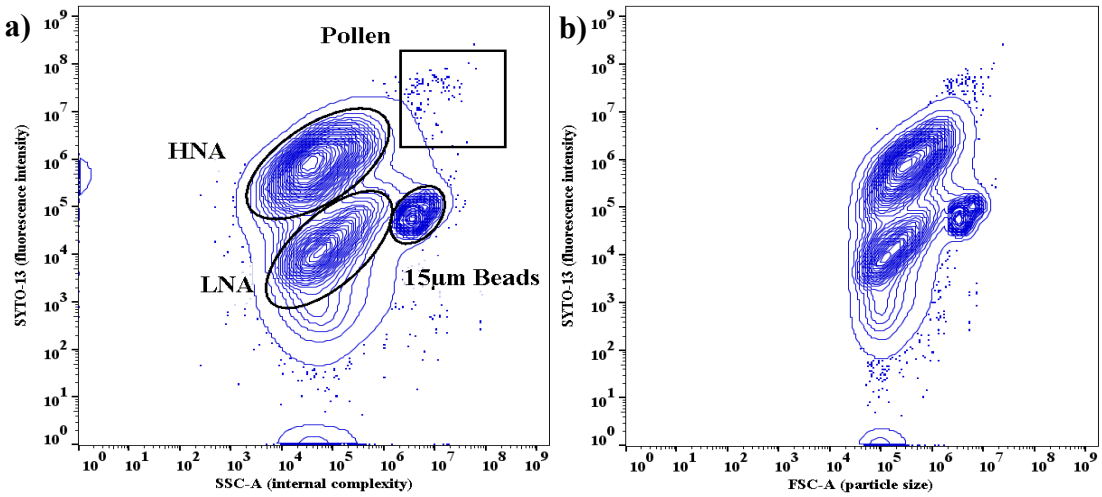

Figure S3: FLI-A vs. SSC-A and FLI-A vs. FSC-A contour plots (example from April 14, 2015 atmospheric sample) used to gate bioaerosol populations using FlowJo maximum resolution (2% contour plots).

SI.4 WIBS-4A sampling losses calculations

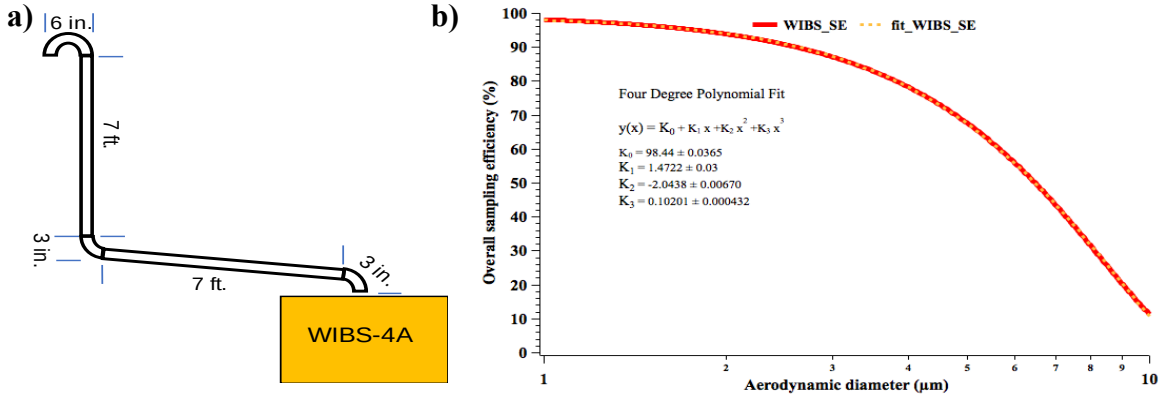

Figure S4: WIBS-4A modeled 15 ft. sampling line in (a) and Particle Losses Calculator overall sampling efficiency results in the 1 to 10 µm size range.

WIBS-4A overall sampling losses for the setup describe in FigureS4a were constrained using the Particle Losses Calculator (PLC) developed by Von der Weiden et al., 2009 calculating the overall sampling efficiency (OSE; aspiration efficiency + transport efficiency). The setup is described as a 5 tubing sections with a 6.35 mm (1/4 in.) inner diameter (ID); 2.3 L min^{-1} flow rate and unit density (1,000 Kg m^{-3}) were also provided as inputs to the model. The output of the model is plotted in Figure S4b (red line) for 1 to 10µm aerodynamic particle sizes. Then, 4hr averaged size distributions were generated for WIBS total particle concentration and all FBAP type categories from 1 to 10µm. The size distributions were generated using as reference the biggest size in each bin (upper bound). For instance, if a particle is between 0.9 µm and 1 µm it will be counted as part of the 1µm bin, and 100 bins were used between 0.1µm and 10µm. Subsequently, a four-degree polynomial regression was applied to the PLC data (Figure S4b) and the equation given by the fit was used to correct WIBS-4A uncorrected size distributions using the midpoint of each bin as the average size to calculate the OSE (e.g. particles in a bin between 1.0 and 1.1 µm will use 1.05µm as the average size to calculate the OSE). In addition, throughout the process of correcting WIBS-4A losses the aerodynamic diameter calculated by PLC is considered equivalent to the optical particle diameter calculated by the WIBS-4A assuming aerosol particles have unit density and understanding that WIBS-4A considers all particles spheres when Mie Scattering approach is applied to calculate aerosol size. The general equation used to correct each bin of the WIBS-4A size distributions is given by:

$$WIBS\ corrected\ \ bin\ (i) = [WIBS\ uncorrected\ bin(i)] * \left[\frac{100}{OSE(i)}\right] \qquad S2$$

where *i* represents each of the size bins in the size distribution (e.g. i=1,2,3…100) and OSE *(i)* is the overall sampling efficiency calculated for each size bin.

SI.5 SEM pictures

1mL of atmospheric sample was filtered through a 0.2µm Nucleopore filter for each sample. The filters were attached to 25mm mounters and coated with a Gold/Carbon sputter. Then, pictures were taken using a LEO 1530 Thermally-Assisted Field Emission (TFE) Scanning Electron Microscope (SEM).

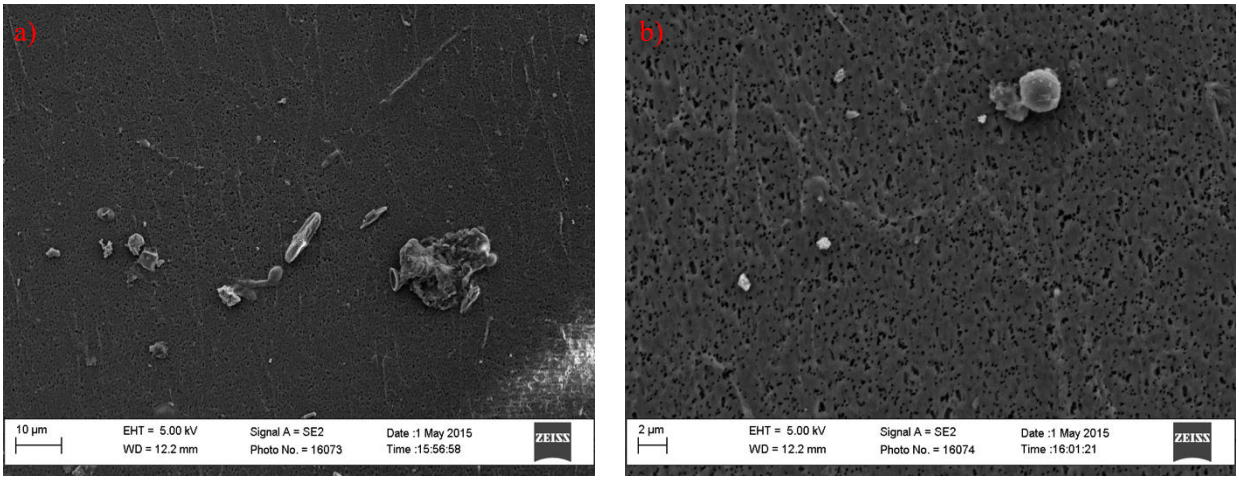

Figure S5a-b: Scanning Electron Microscope (SEM) pictures taken of April 14, 2015 SpinCon II sample. a) shows a heterogeneous population of particles including: dust, bacteria, fungal spores and other particles; b) shows small dust particles and a small fungal spore(~2µm).

SI.6 EPM pictures

Epifluorescence microscopy (EPM) pictures were taken during the design of the FCM protocol. We were able to distinguish different types of particles on them like: bacteria, fungal spores and pollen. Samples were stain using the Live/Dead staining kit. The 1mL stained sample was incubated for 15min; then was filtered in a 0.2µm black Isopore filter and placed in a glass slide. Samples were observed in the Axion Observer D1 epifluorescence microscope (Zeiss). As observed in Figure S6 microorganisms show non-intact cell membranes given the presence of propidium iodide (PI) inside them.

Additional EPM pictures were taken of SpinCon II samples collected in September 9-11, 2015, which are not included in this manuscript, but the same FCM protocol was used as in April-May sampling. During these experiments samples were stained with a 20µg/mL DAPI concentration. The 1mL stained sample was incubated for 15min; then was filtered in a 0.2µm black Isopore filter and placed in a glass slide. Samples were observed in the Axion Observer D1 epifluorescence microscope (Zeiss). Samples show a heterogeneous bioaerosol population as seen in Figure S7a. EPM and FCM results were quantitatively compared in September, 2015 samples. EPM quantification was performed taking 20 pictures (5 rows, 5 pictures by row) of a representative area and it was repeated for a total of 3 representative areas (e.g. bottom, middle and top of the filter) within the filter to have an experimental triplicate. Cells were counted in each representative area and the filtrated volume was used to determine the liquid-based concentration for each sampling event. Thin cells smaller than 5µm were considered bacteria and thick cells between 5-10µm were considered fungal spores. Particles larger than 10µm and irregular-shaped particles were categorized as "others" and they constituted a small fraction of the total cells (~5%). The total PBAP EPM-derived concentrations consisted of the sum of bacteria, fungal spores and "others" particles concentrations. FCM biopopulations identification was performed using the protocol described in Section 3.1 and quantified with the same approach used for the April-May 2015 atmospheric samples (supplemental information, SI.8)

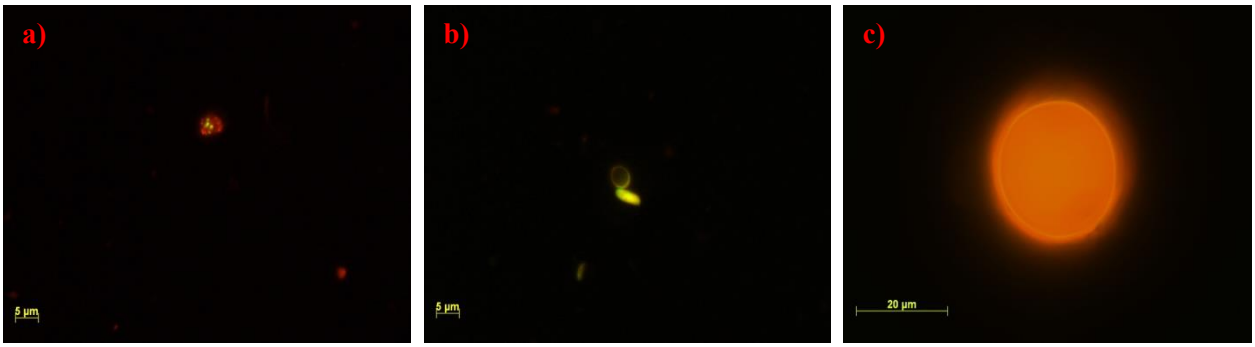

Figure S6a-c: EPM pictures of atmospheric samples collected in March 24, 2015 showing different types of biological particles. a) shows a bacteria agglomerate, b) shows two attached fungal spores and c) shows ~20µm pollen particle.

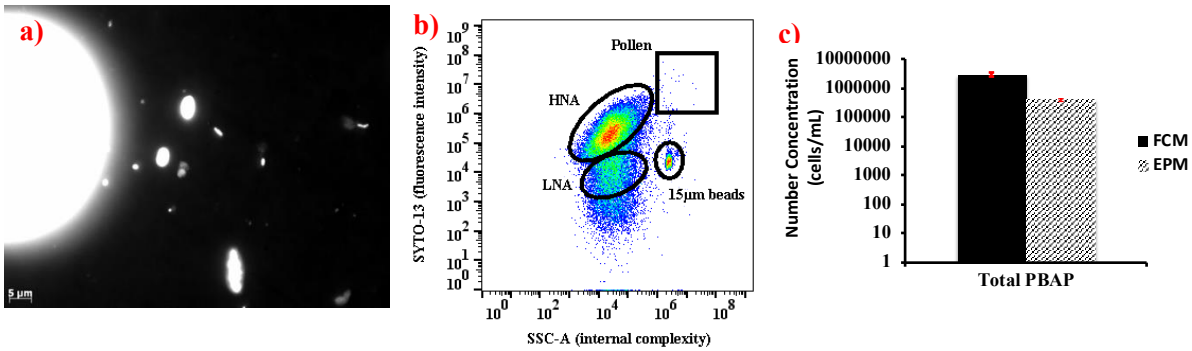

Figure S7a-c: EPM pictures of the September 9, 2015 atmospheric sample (S7a), September 11, 2015 FCM results with identified populations (S7b) and September 11, 2015 EPM and FCM quantitative comparison (S7c).

SI.7 FCM subpopulations particle size determination

The mean size of each population was determined by comparing 1µm, 2µm, 4µm, 6µm, 10µm, 15µm standardize beads (Flow Cytometry calibration kit, Life Technology Inc.) FSC-A scattering distributions with the populations FSC-A scattering distributions. First, standardized beads were analyzed in triplicate by FCM. Then the geometric mean FSC-A intensities were calculated for each bead size (using FlowJo). Two samples were prepared: a) having 10µL of 1µm, 4µm and 10µm beads; and b) having 10µL of 2µm, 6µm and 15µm beads; both diluted to 1mL with Milli-Q water. Samples SSC-A vs. FSC-A plots are shown in Figure S8a-b.

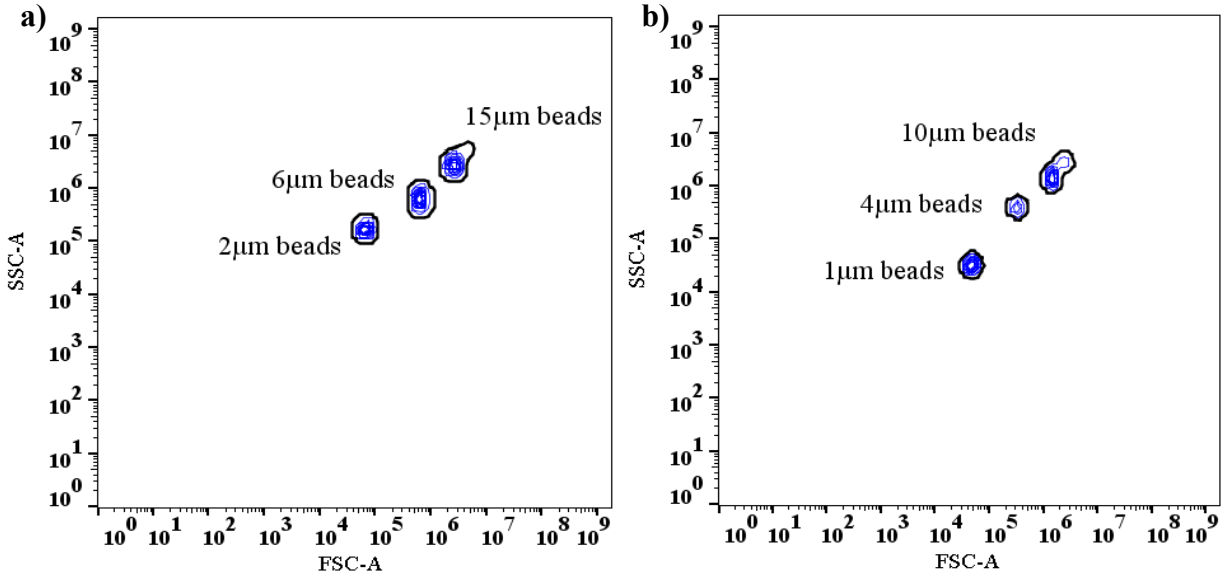

Figure S8a-b: SSC-A vs. FSC-A plots of the FCM calibration beads experiments showing the different type of beads used for size calculations.

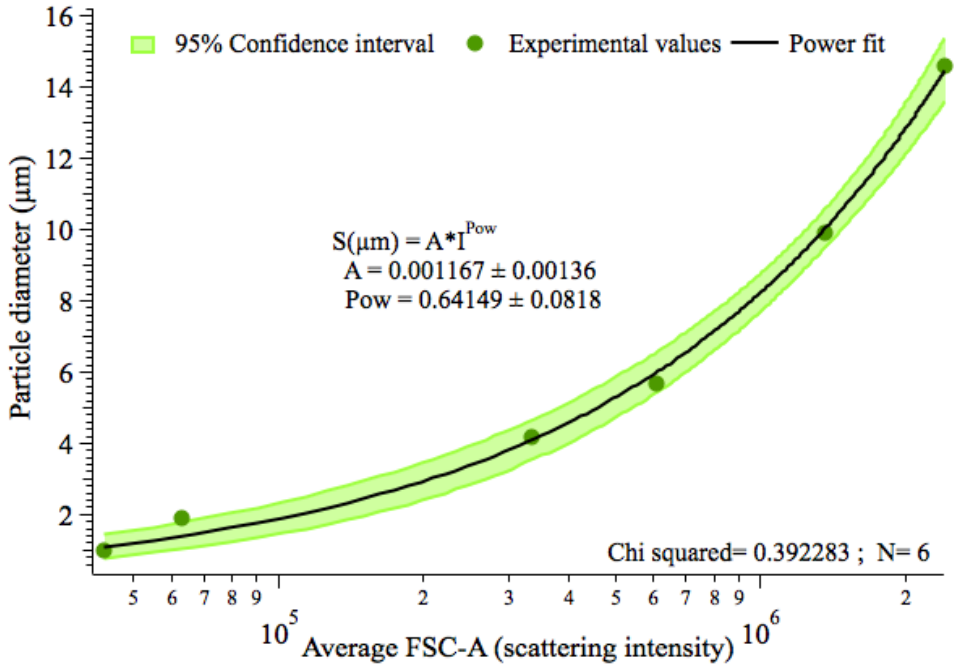

Figure S9: Plot used to determine the subpopulations mean size. Results of the FCM analysis of the calibration beads. X axis is in logarithmic scale.

Then a power regression, shown in Figure S9, was performed to the beads size vs. beads FSC-A fluorescence intensity plot to get an equation to relate beads particle size (diameter) and its respective geometric mean FSC-A intensity.

Based on the regression, the following equation was used to calculate the size of each particle detected by FCM:

$$S(\mu m) = 0.001167\, I^{0.64149} \qquad [S3]$$

where S is the mean size of the particle in µm and I is the averaged geometric mean FSC-A intensity of the particle. The equation calculated the mean size of each particle detected by FCM successfully, but it may have overestimated pollen size given the extrapolation performed to apply the equation to bigger particles (above 15µm diameter). Then, the mean diameter of each FCM population was calculated applying a Gaussian Fit to the geometrically averaged size distributions generated for all SpinCon II sampling events (Figure S10). Results summarized in Table S1 describe mean sizes of each population during April-May sampling events(n=15)

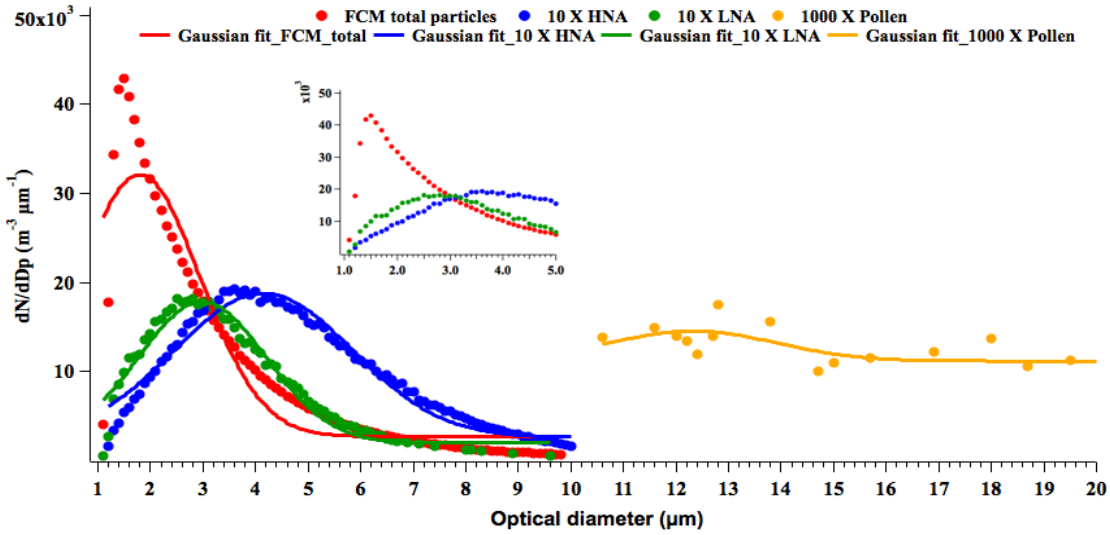

Figure S10: FCM total particles, HNA, LNA and Pollen size distributions (geometric averaged over the 15 SpinCon II sampling events) and Gaussian fits applied to each size distribution to determine the mean diameter of each population.

Table S1: Summary of the mean size (calculated from Gaussian fits in Figure 10) of the FCM total particles and the identified bioparticle populations during SpinCon II sampling events(n=15) . *No collection efficiency (ABC correction factor) applied within this calculation.

	FCM total particles	LNA	HNA	Pollen
Mean diameter (µm)	1.7909	2.9854	4.1506	12.32
Standard deviation (µm)	0.214	0.0638	0.0621	1.67
CV%	12.0%	2.1%	1.5%	13.1%

SI.7 Pollen Autofluorescence

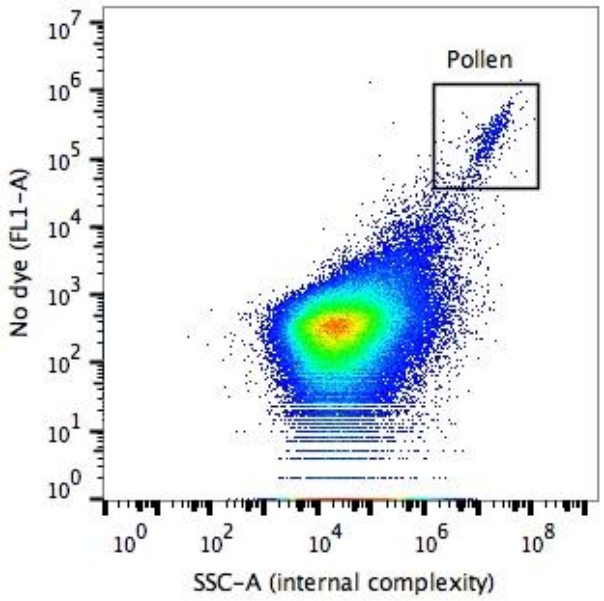

Figure S11: FCM pollen autofluorescence in the atmospheric sample without SYTO-13.

SI.8 FCM PBAP quantification

Equation S4 was used to calculate the liquid-based concentration ($\mathbf{C_{liq}}$) for each FCM-identified bioaerosols population and the total PBAP in the atmospheric and pure culture samples, which is a modification to Lange et al., 1997 quantification equation:

$$\boldsymbol{C_{liq}} = \left(\frac{A * C}{0.99 * B}\right) \quad [S4]$$

where *A* refers to the population counts above the 42k threshold (41,839 FL1_A units) given by FlowJo, *B* refers to the volume of the aliquot of sample (mL) used for the FCM analysis and C refers to the inverse of the counting efficiency (ϵ) which is given by:

$$C = \left(\frac{1}{\epsilon}\right) = \left(\frac{beads\ added\ volume \times beads\ original\ concentration}{counts\ given\ by\ flow\ Jo}\right) \quad [S5]$$

The 0.99 factor in equation S4 takes in consideration the 10 µL of 37 wt.% formalin added to the original sample, representing a 1% dilution of the atmospheric sample aliquot. Beads original

concentration during these experiments was 2 x 10^7 beads/mL. Then, equation S6 was applied to compute the uncorrected air-based concentration of each population $\mathbf{C_{air}}$:

$$\boldsymbol{C_{air}} = \left(\frac{C_{liq} * D}{E * F}\right) \quad [S6]$$

where *D* refers to the collected sample total volume (mL), *E* refers to the SpinCon II volumetric flow rate (478 L min^{-1} or 0.478 m^3 min^{-1}) and *F* refers to the atmospheric sample sampling time (min).

Finally, the total uncorrected air-based PBAP concentration (m^{-3}) for each sampling event was calculated based on the total particle counts above the 42k threshold value using equations S4, S5, and S6. The quantification of the "unclassified biological" (**UBIO**), biological particles not constrained by gaiting procedure, was performed using the following equation:

$$\boldsymbol{UBIO}\ (m^{-3}) = Total\ PBAP(m^{-3}) - bioLNA(m^{-3}) - HNA(m^{-3}) - Pollen(m^{-3}) \quad [S7]$$

SI.9 HNA and ABC populations correlation

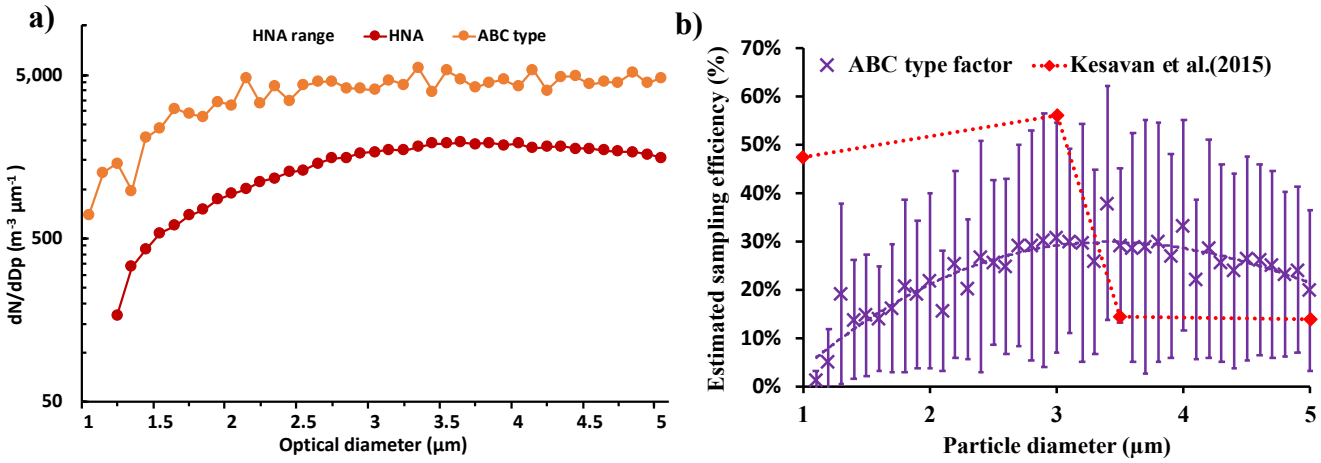

Figure S12: a) FCM HNA and WIBS ABC types 1 to 5µm size distributions (geometrically averaged) comparison including the range (defined by the geometric standard deviation) of HNA size distributions over the 15 SpinCon II sampling events; b) Estimated sampling efficiency (ECE) comparison to Kesavan et al., 2015 sampling efficiencies for SpinCon I.

FCM correction factors (CF) are based on WIBS-4A ABC type and FCM HNA size distributions in the 1 to 5µm range for each SpinCon II sampling day. CF were calculated for each day the HNA population was identified (n=12) and for the rest of the days (n=3) averaged CF values were used to correct FCM concentrations. FCM size distributions were generated using the same approach used for WIBS-4A (described in SI.4) and FCM particle size was calculated using equation S3. The CF calculations were performed for each bin within the 1 to 5µm range and CF is given by the following equation:

$$CF\ (i) = \left(\frac{\text{ABC corrected bin (i)}}{\text{HNA uncorrected bin (i)}}\right) \quad [S8]$$

where *i* represents each of the bins between 1 to 5µm range in the size distribution. Then, CF for each bin was multiplied by the HNA, bioLNA, total PBAP and total particle size distributions to calculate the FCM corrected size distributions. From the corrected size distributions, the number concentration on each bin was acquired and the total corrected concentration in each population constituted the sum of the number concentrations of all bins between 1 to 5µm. In addition, unclassified biological concentrations (UBIO) were calculated using equation S7, but with the FCM corrected concentrations. Finally, the estimated sampling efficiency (ECE) plotted in Figure S12b is given by the following equation:

$$ECE(i) = \frac{100}{CF(i)} \quad [S9]$$

where *i* represents each of the bins between 1 to 5µm range in the size distribution.

SI.10 FCM Pure Cultures experiments

Pure culture experiments were performed during the study as an additional support to the observations seen in the atmospheric samples. Two different types of experiments were conducted: i) the individual microorganisms (bacteria, yeast and pollen) were analyzed to visualize the population of microorganisms; ii) mixtures of the microorganisms were analyzed to understand how they would look all together and see how it compares with what is seen in the atmospheric samples.

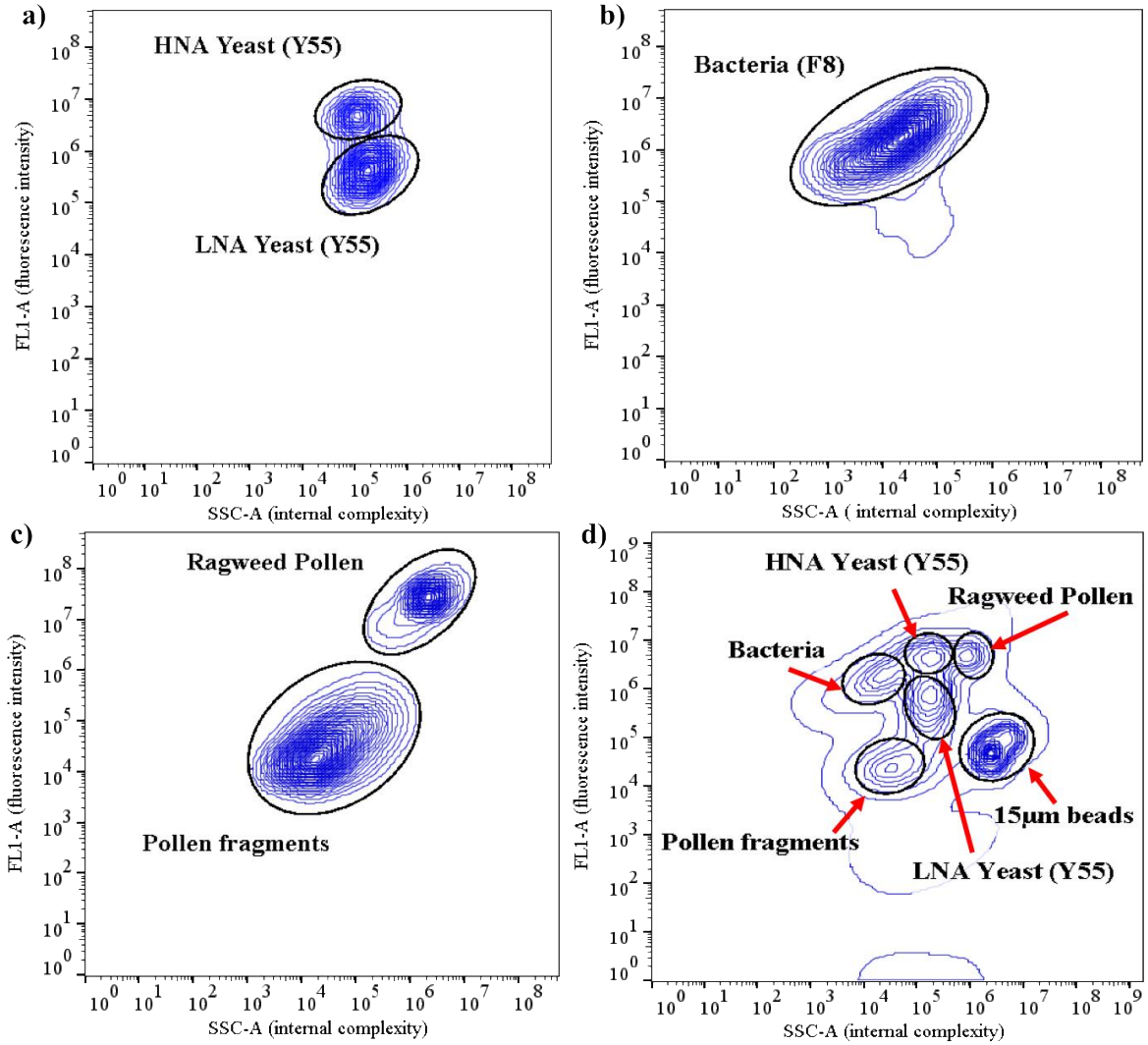

Figure S13: FCM pure culture FL1-A vs. SSC-A plots. a), b) and c) show FCM results of individual yeast isolate (Y55 strain), bacteria atmospheric isolate (F8), and Ragweed pollen, respectively; and d) shows FCM results of the mixture of microorganisms.

Yeast (Y55) and Bacteria (F8) strains used in the experiments were grown overnight in non-limited oxygen conditions. Y55 was grown in 1X yeast extract at 35°C and F8 was grown in 1X LB broth at 30°C. Then an aliquot of each was fixed with formalin. Ragweed pollen (Ambrosia artemisiifolia), purchased to Greer Laboratories (Lenoir, NC), was used without further purification. A 10mg/mL pollen/PBS solution was prepared as working stock. Then different dilutions were performed to yeast, bacteria and pollen samples to reach 10^4-10^5 part. /mL concentration and were individually analyzed by FCM. Figure S13a-c show the results of the individual microbial populations. Then mixtures of the microorganisms were analyzed using the

same SYTO-13 and 15µm beads concentrations used for the atmospheric samples. Results in Figure S13d show populations are close to each other given their similar sizes and internal complexities. Also, microorganism populations show higher SYTO-13 fluorescence intensity than those in the atmospheric samples, as it observed in Figure S13a-d and summarized in Table S2. Among mixed populations experiments we focused in the pollen to pollen fragments ratio given pollen fragments importance in the atmospheric sample bacteria quantification. Based on the results, a 1.1 x 10^4 part. /mL pollen population will release 2.7 x 10^4 part. /mL of pollen fragments when is in contact with aqueous solution, which constitute approximately a 1 to 2.4 ratio (Look Table S2). Given the small pollen concentration seen in the atmospheric samples, it is understood the impact of pollen fragmentation in bioLNA quantification will be negligible.

Table S2: Pure cultures triplicate concentrations overview.

PBAP Type	Pure Culture Triplicates			Average (mL^{-1})	Standard Deviation (mL^{-1})	CV (%)
	SC1880	SC1881	SC1882			
Pollen	1.20×10^4	1.04×10^4	1.05×10^4	1.09×10^4	8.96×10^2	8.2%
Pollen Fragments	2.92×10^4	2.27×10^4	2.78×10^4	2.66×10^4	3.41×10^3	12.8%
Bacteria	1.99×10^4	1.75×10^4	1.55×10^4	1.76×10^4	2.23×10^3	12.6%
HNA Yeast	2.61×10^4	2.45×10^4	2.57×10^4	2.54×10^4	8.37×10^2	3.3%
LNA Yeast	4.09×10^4	4.25×10^4	3.65×10^4	4.00×10^4	3.13×10^3	7.8%

Pure culture and atmospheric samples FSC-A, SSC-A and FL-1 properties, summarized in Table S3 and Table S4, show interesting differences in their fluorescence intensities, possibly related to a reduction in the genetic content of atmospheric microorganisms due to starvation.

Table S2: Pure cultures mixture FSC-A, SSC-A and FL1-A properties summary.

PBAP Type	FSC-A Avg.	FSC-A SD	SSC_A Avg.	SSC-A SD	FL1-A	FL1-A SD
Bacteria	7.23×10^4	8.54×10^3	1.52×10^4	2.67×10^3	1.30×10^6	1.81×10^5
HNA yeast	6.03×10^5	1.06×10^4	1.45×10^5	9.44×10^3	4.04×10^6	1.66×10^5
LNA yeast	1.17×10^6	2.29×10^4	1.61×10^5	4.09×10^3	6.16×10^5	1.43×10^5
Pollen	5.03×10^5	9.33×10^4	8.72×10^5	3.94×10^4	4.21×10^6	2.51×10^5
Pollen fragments	7.54×10^4	4.77×10^3	4.27×10^4	1.44×10^4	2.47×10^4	8.46×10^2

Table S3: Atmospheric populations FSC-A, SSC-A and FL-1 properties summary of SpinCon II sampling events (n=15) during April-May, 2015.

	bioLNA Geo Mean			HNA Geo Mean			Pollen Geo Mean			Beads Geo Mean		
	FSC-A	SSC-A	FL1-A	FSC-A	SSC-A	FL1-A	FSC-A	SSC-A	FL1-A	FSC-A	SSC-A	FL1-A
Average	2.67×10^5	1.40×10^5	7.38×10^4	3.89×10^5	7.87×10^4	6.72×10^5	3.50×10^6	5.88×10^6	6.57×10^6	3.02×10^6	3.28×10^6	5.87×10^4
SD	8.19×10^4	6.91×10^4	1.39×10^4	8.42×10^4	3.00×10^4	2.30×10^5	2.86×10^6	5.85×10^6	2.85×10^6	6.47×10^5	7.73×10^5	4.39×10^4
Max	4.52×10^5	2.71×10^5	1.00×10^5	4.84×10^5	1.08×10^5	1.08×10^6	1.32×10^7	2.62×10^7	1.35×10^7	3.95×10^6	4.59×10^6	1.80×10^5
Min	1.36×10^5	4.71×10^4	5.19×10^4	1.99×10^5	2.48×10^4	3.11×10^5	1.68×10^6	2.73×10^6	2.87×10^6	1.69×10^6	1.85×10^6	1.46×10^4

SI.11 Arizona Test Dust (ATD) FCM Experiments

Experiment using unprocessed and commercially available (Powder Technologies Inc.) Arizona Test Dust (ATD) were conducted by suspending ATD in 1X PBS. 20mg of the ATD were diluted into 10mL of PBS and fixed with 1 vol.% formalin overnight. Then, a 1/20 dilution of the initial ATD solution was filtered through a sterile 10µm pore size Isopore filter (Millipore Sigma) to prevent clogging the flow cytometer with big particles. Subsequently, ATD was stained with 2.5 µM SYTO-13 (same concentration used to stain the atmospheric samples) and incubated in the dark at room temperature for 15 min. before been analyzed by Flow Cytometry. Histograms of the analyzed ATD solutions (~10^6 particles mL^{-1}) below show the fluorescence intensity (FL1-A intensity) distributions of unstained (Figure S14a, blue) and stained ATD (Figure S14b, orange) particles are negligibly different, and 100% of the stained ATD particles have a FL1_A intensity below the threshold value (41,839) used to distinguish between abiotic and biotic particles. ATD results support SYTO-13 does not bind to abiotic particles and agree the applied fluorescence threshold effectively filters out abiotic particles.

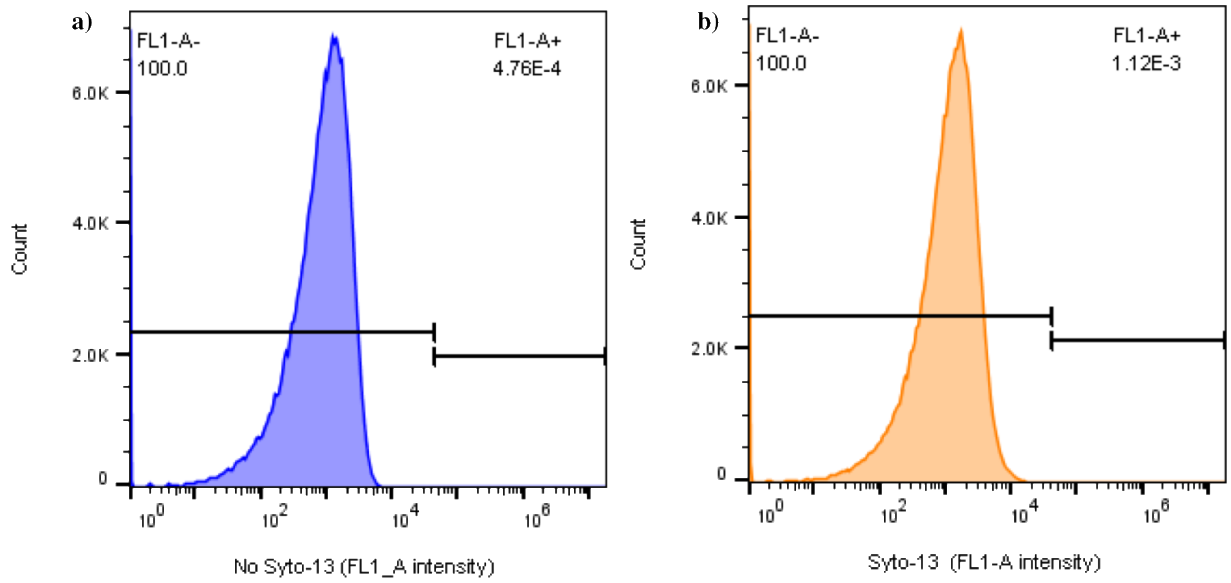

Figure S14: ATD FL1_A intensity histogram distributions for unstained (a) and (b) stained ATD, where FL1_A- and FL1_A+ subpopulations represent the percentage of particles with FL1_A intensity above and below the fluorescence intensity threshold value (41,839), respectively.

SI.12 FCM plots for SpinCon II sampling events

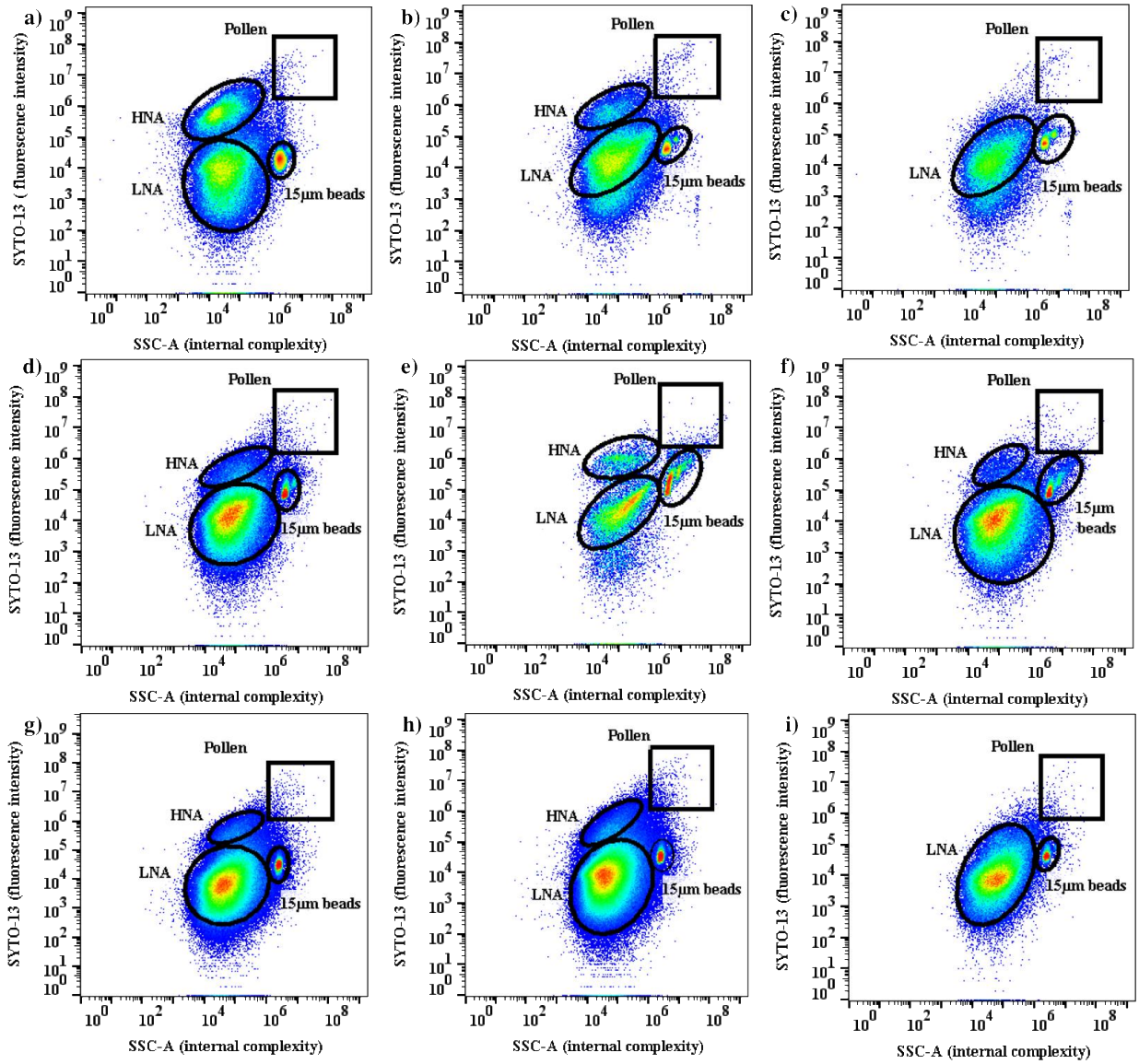

Figure S15a-i: FCM FL1-A vs. SSC-A plots (pseudo-color plots show higher particle accumulation in green to red regions) for the following 2015 April-May SpinCon II sampling events: a) April 7, b) April 8, c) April 9, d) April 28, e) April 29, f) April 30, g) May 13, h) May 14 and i) May 15.

SI. 13 1.0µm polystyrene beads cutoff test

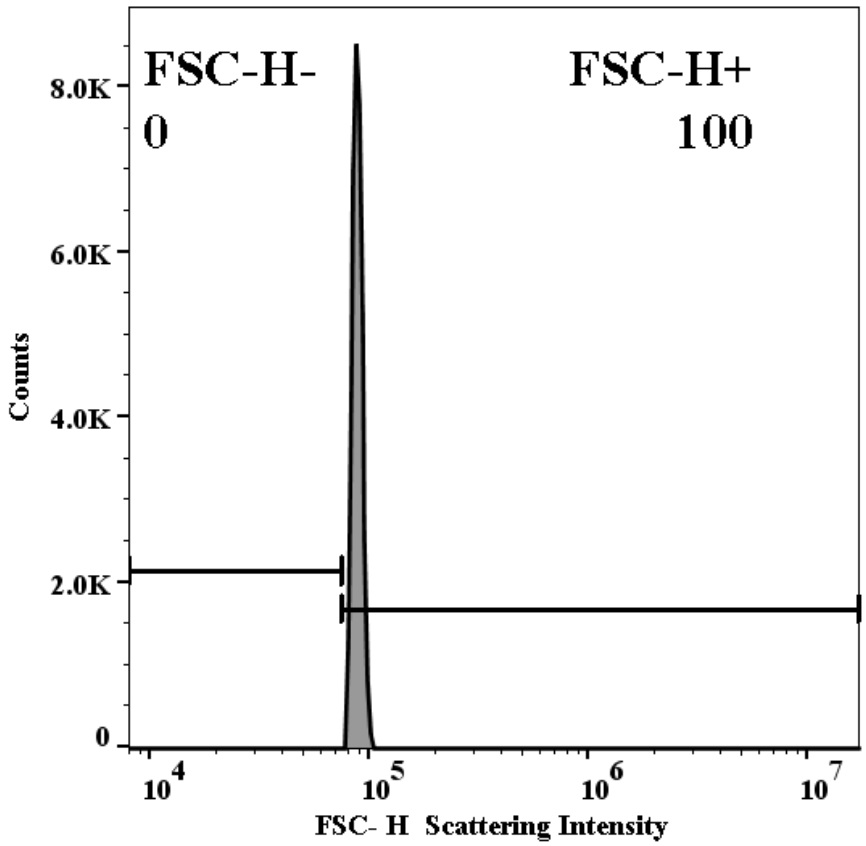

Figure S16: 1.0µm polystyrene beads histogram showing the totality of them have FSC-H scattering intensities above the 80,000 units. Experiment performed using the FSC-H default threshold and concentrations agree to that provided by the manufacturer.

SI. 14 WIBS total particle concentration vs. FBAP types correlation

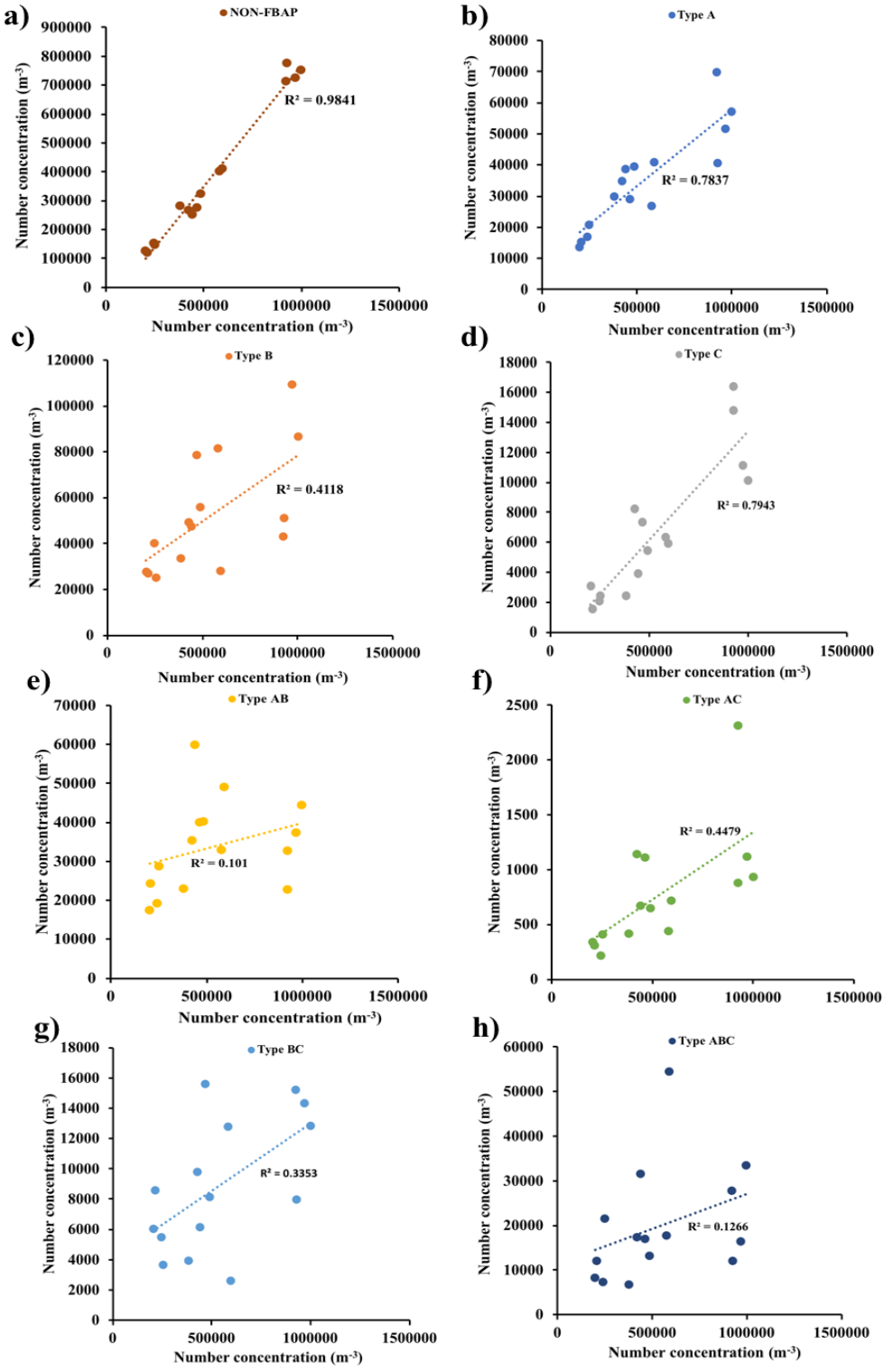

Figure S17: 4h averaged WIBS total particle concentration comparison to FBAP types concentration including: a) NON-FBAP, b) Type A, c) Type B, d) Type C, e) Type AB , f) Type AC, g) Type BC and h) Type ABC.

SI. 15 WIBS corrected, FCM uncorrected and FCM corrected total concentration variability

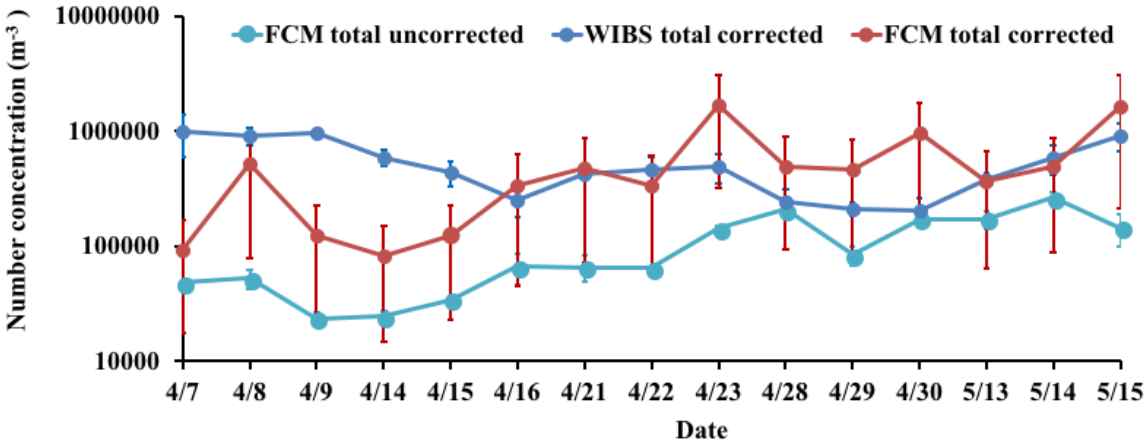

Figure S18: WIBS corrected total particle concentration (4 hr. avg.), FCM uncorrected concentration and FCM corrected (using ABC size distributions) concentration variability between April 7 to May 15, 2015

SI.16 Type B and bioLNA anticorrelation

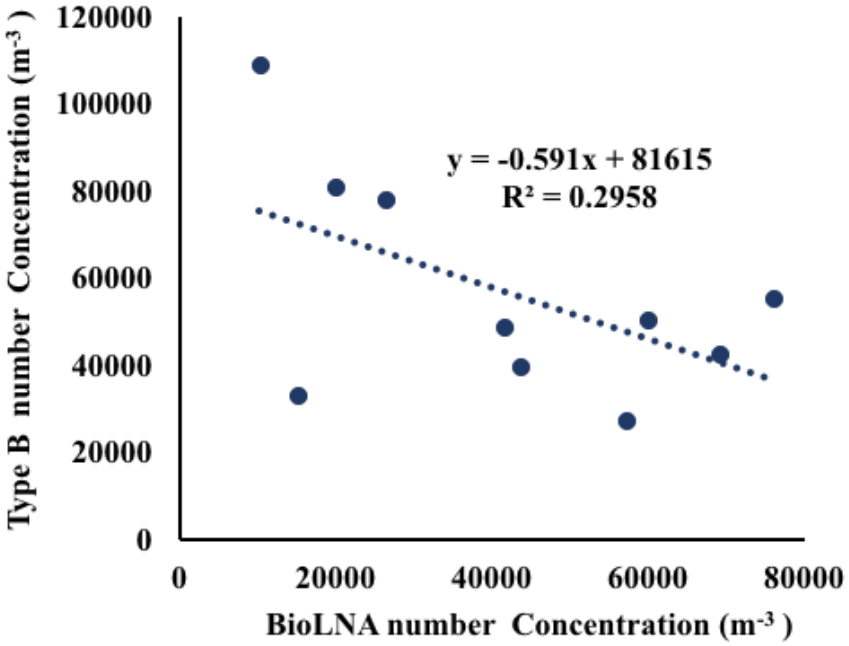

Figure S19: Type B and bioLNA number concentration anti-correlation on dry days (n=10)

SI. 17 WIBS total particle vs. Jefferson St. PM10 mass

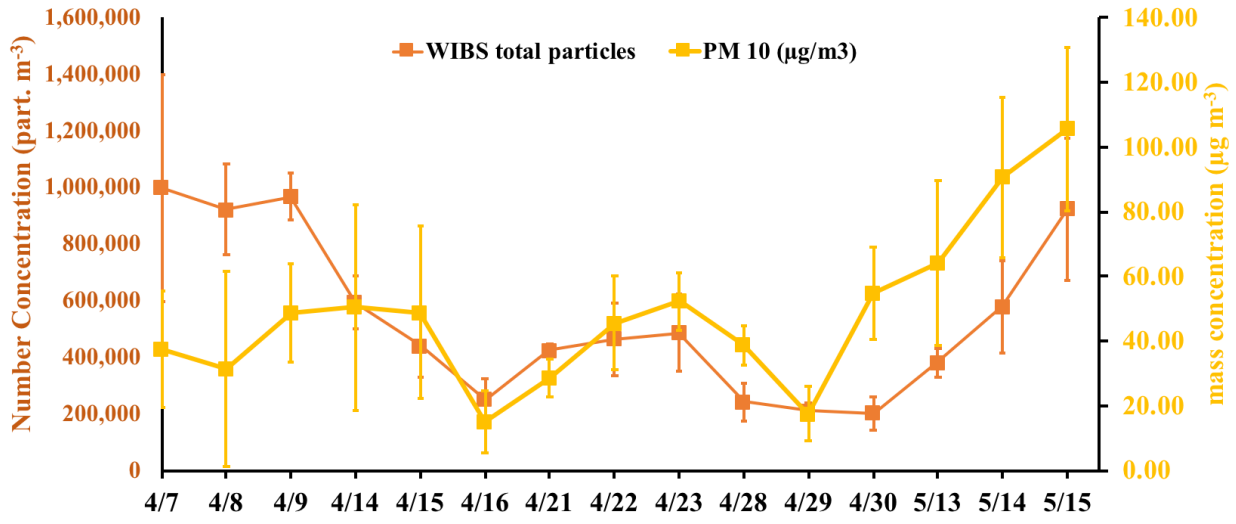

Figure S20: 4h averaged WIBS total particle concentration (left Y axis) and PM_{10} mass concentration (right Y axis) for each SpinCon II sampling event.

SI.18 Meteorological Data

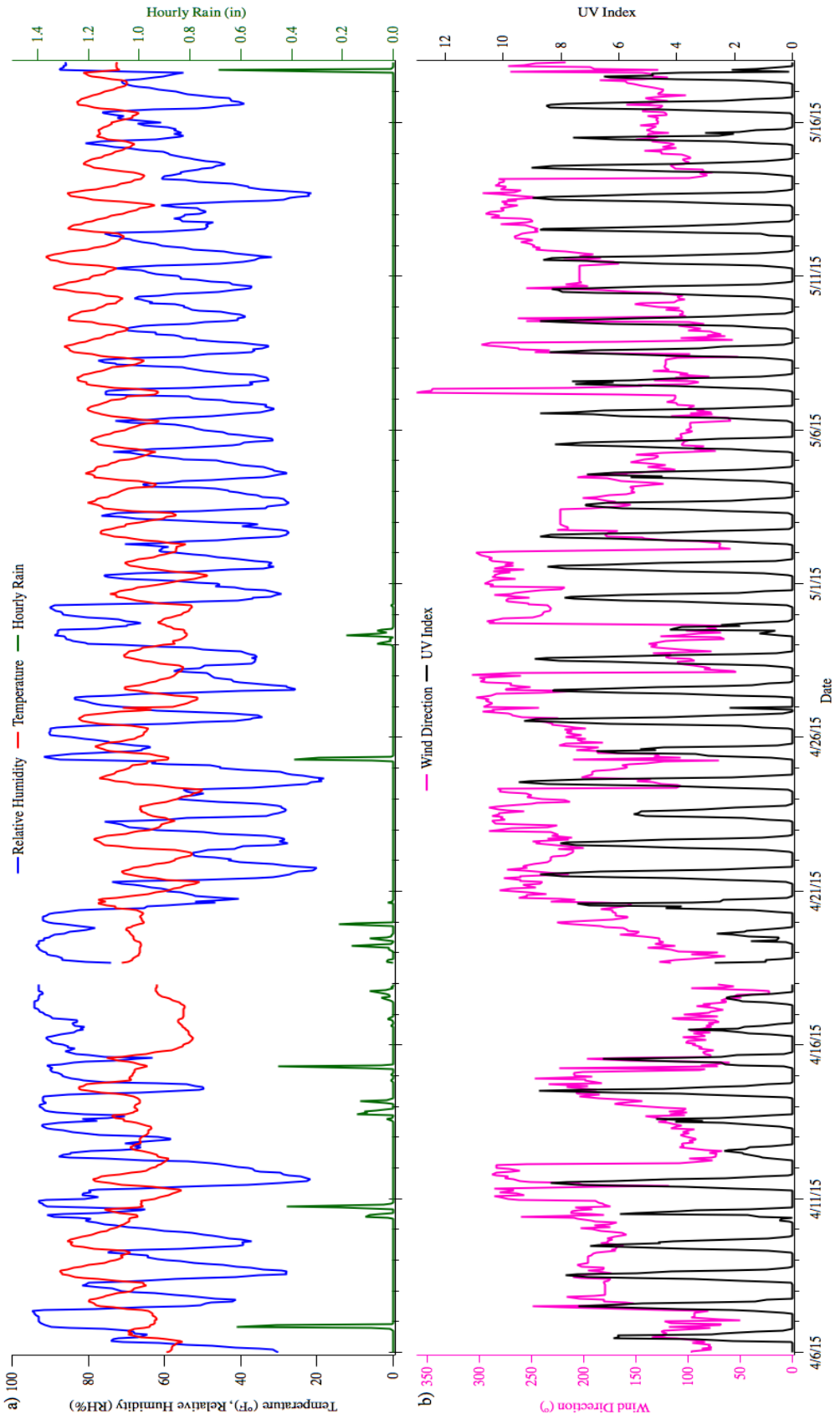

Figure S21: April-May meteorological data summary (hourly averages). Includes relative humidity, temperature, hourly rain, wind direction and UV index